Developmental Cell
Article

Calpain 2 Activation of P-TEFb Drives Megakaryocyte Morphogenesis and Is Disrupted by Leukemogenic GATA1 Mutation

Kamaleldin E. Elagib,[1] Jeremy D. Rubinstein,[1] Lorrie L. Delehanty,[1] Valerie S. Ngoh,[1] Peter A. Greer,[2] Shuran Li,[3] Jae K. Lee,[3] Zhe Li,[4,5] Stuart H. Orkin,[4,5] Ivailo S. Mihaylov,[1] and Adam N. Goldfarb[1,*]
[1]Department of Pathology, University of Virginia School of Medicine, Charlottesville, VA 22908, USA
[2]Department of Pathology and Molecular Medicine, Queen's University, Kingston, Ontario K7L 3N6, Canada
[3]Department of Public Health Sciences, University of Virginia School of Medicine, Charlottesville, VA 22908, USA
[4]Division of Hematology/Oncology, Children's Hospital Boston, Harvard Stem Cell Institute, Harvard Medical School, Boston, MA 02115, USA
[5]Department of Pediatric Oncology, Dana-Farber Cancer Institute, Harvard Stem Cell Institute, Harvard Medical School, Boston, MA 02115, USA
*Correspondence: ang3x@virginia.edu
http://dx.doi.org/10.1016/j.devcel.2013.11.013

SUMMARY

Megakaryocyte morphogenesis employs a "hypertrophy-like" developmental program that is dependent on P-TEFb kinase activation and cytoskeletal remodeling. P-TEFb activation classically occurs by a feedback-regulated process of signal-induced, reversible release of active Cdk9-cyclin T modules from large, inactive 7SK small nuclear ribonucleoprotein particle (snRNP) complexes. Here, we have identified an alternative pathway of irreversible P-TEFb activation in megakaryopoiesis that is mediated by dissolution of the 7SK snRNP complex. In this pathway, calpain 2 cleavage of the core 7SK snRNP component MePCE promoted P-TEFb release and consequent upregulation of a cohort of cytoskeleton remodeling factors, including α-actinin-1. In a subset of human megakaryocytic leukemias, the transcription factor GATA1 undergoes truncating mutation (GATA1s). Here, we linked the GATA1s mutation to defects in megakaryocytic upregulation of calpain 2 and of P-TEFb-dependent cytoskeletal remodeling factors. Restoring calpain 2 expression in GATA1s mutant megakaryocytes rescued normal development, implicating this morphogenetic pathway as a target in human leukemogenesis.

INTRODUCTION

Mammalian hematopoietic differentiation proceeds by a series of binary decisions that yield progenitors of increasingly limited developmental potential, with the megakaryocyte lineage emerging from a bipotent megakaryocyte-erythroid progenitor (MEP). Megakaryocytic and erythroid cells, despite common origins, shared transcription factors, and shared signaling pathways, differ profoundly in their developmental programs. Erythroid morphogenesis occurs through progressive reduction in cell size accompanied by nuclear condensation and ultimately extrusion. Megakaryocytic morphogenesis contrastingly involves marked expansion in cell mass combined with acquisition of a lobulated, polyploid nucleus containing up to *32-64N*. In this regard, megakaryopoiesis bears resemblance to the program of cardiomyocyte hypertrophy, in which pressure overload elicits cellular enlargement and polyploidization (Liu et al., 2010).

Mechanistically, the developmental morphogenesis of megakaryocytes and the hypertrophic response of cardiomyocytes share key regulatory elements. At the transcriptional level, both programs rely on a complex of serum response factor (SRF) with myocardin-related transcription factors (Cheng et al., 2009; Halene et al., 2010; Kuwahara et al., 2010; Nelson et al., 2005; Smith et al., 2012), as well as on MEF2C (Gekas et al., 2009; Muñoz et al., 2009). At the signaling level, both programs require high-amplitude activation of the P-TEFb kinase pathway (Elagib et al., 2008; Sano et al., 2002). A critical distinction is that cardiomyocyte hypertrophy consists of a reversible response to a pathologic stimulus, whereas normal megakaryocyte morphogenesis represents an irreversible, terminal program largely driven by cell-intrinsic mechanisms.

Cellular P-TEFb kinase activity is tightly regulated, with the majority of the Cdk9-cyclin T kinase modules sequestered in large inactive complexes containing the 7SK snRNA, HEXIM1, MePCE, LARP7, and additional factors (Barboric et al., 2009; Jeronimo et al., 2007; Peterlin and Price, 2006; Price, 2008; Xue et al., 2010). Several stimuli, including hypertrophic agonists (e.g., endothelin-1), UV irradiation, HIV-1 Tat, and hexamethylene bisacetamide activate P-TEFb by inducing the release of Cdk9-cyclin T from the 7SK small nuclear ribonucleoprotein particle (snRNP) complex (Chen et al., 2008; Contreras et al., 2007; Krueger et al., 2010; Sano et al., 2002; Sano and Schneider, 2004). These stimuli variously trigger signaling via Gq, calcineurin, PP1α, and PI3K, ultimately leading to remodeling of the 7SK snRNP that promotes dissociation of Cdk9-cyclin T and HEXIM1 away from the stable core complex of 7SK, MePCE, and LARP7. Once activated, P-TEFb promotes transcriptional elongation by phosphorylating RNA polymerase II and associated pausing factors. Feedback autoregulation results from the rapid and potent induction of *HEXIM1* transcription

(Bartholomeeusen et al., 2012; Garriga et al., 2010; He et al., 2006), effectively driving resequestration of Cdk9-cyclin T back into an inactive 7SK snRNP complex (Bartholomeeusen et al., 2012; Zhou et al., 2012).

GATA1, a master transcriptional regulator of megakaryocyte and erythroid differentiation, physically and functionally interacts with P-TEFb in hematopoietic cells (Bottardi et al., 2011; Elagib et al., 2008). Somatic mutations yielding an N-terminal truncated, "short" GATA1 protein (GATA1s) occur in virtually all megakaryocytic neoplasms associated with Down syndrome (Wickrema and Crispino, 2007). In knockin mice, the mutant GATA1s induces transient megakaryocytic hyperproliferation and maturational defects during fetal liver hematopoiesis (Li et al., 2005). Megakaryocytic hyperproliferation and aberrant differentiation have also been elicited by P-TEFb inhibition in adult mice with megakaryocytic GATA1 deficiency, supporting the notion of a GATA1-P-TEFb megakaryopoietic pathway that might be affected in Down syndrome neoplasms (Elagib et al., 2008).

In the current study, we have identified a megakaryopoietic P-TEFb activation pathway characterized by downregulation of the 7SK snRNP core components MePCE, LARP7, and 7SK snRNA. The protease calpain 2 critically participated in this pathway, undergoing recruitment to P-TEFb, targeting MePCE for proteolysis, and promoting P-TEFb-dependent megakaryocyte morphogenesis. A cohort of coregulated cytoskeletal remodeling factors involved in execution of the morphogenetic program was identified in this pathway downstream of P-TEFb. In a large panel of human megakaryocytic leukemias, decreased calpain 2 levels significantly correlated with the presence of the GATA1s mutation. In addition, murine fetal liver megakaryocytes from GATA1s knockin mice displayed defects in upregulation of calpain 2 and of downstream cytoskeletal remodeling factors. Lentiviral restoration of calpain 2 expression specifically ameliorated developmental defects in GATA1s knockin fetal megakaryocytes. These findings thus support a megakaryocyte morphogenetic pathway involving GATA1, calpain 2, P-TEFb, and the actin cytoskeleton. Perturbations of this pathway may play a role in the pathogenesis of Down syndrome megakaryocytic neoplasms.

RESULTS

Global P-TEFb Activation in Megakaryopoiesis

Previous work has suggested a critical role for high-amplitude P-TEFb activation in megakaryocyte differentiation and divergence from the erythroid lineage (Elagib et al., 2008). To examine the mechanistic basis for this activation, 7SK snRNP complex components were quantified in megakaryocytic, erythroid, and undifferentiated cells derived from primary human hematopoietic progenitors. The principal P-TEFb factors in hematopoietic cells, Cdk9 and cyclin T1, showed similar protein levels in megakaryocytic (Mk), undifferentiated (Un), and erythroid (Ery) cells (Figure 1A). By contrast, megakaryocytic cells specifically downregulated all of the components of the recently defined (Barboric et al., 2009; Xue et al., 2010) 7SK snRNP core complex: MePCE (Me), LARP7 (L7), and the 7SK snRNA (Figures 1A and 1B). Additionally, megakaryocytic cells displayed enhanced phosphorylation of RNA polymerase II carboxy terminal domain serine 2 (RNAPII S2), a specific target of P-TEFb phosphorylation (Peterlin and Price, 2006) (Figure 1C). Concomitant with downregulation of the 7SK inhibitory scaffold, megakaryocytes specifically upregulated HEXIM1, reflecting increased cellular P-TEFb activity (Bartholomeeusen et al., 2012; Garriga et al., 2010; He et al., 2006) (Figure 1A). The megakaryocytic induction of HEXIM1 occurred at the mRNA level (Figure S1A available online) and was prevented by the Cdk9 inhibitor flavopiridol (FP) and by shRNA knockdown of Cdk9 (Figure S1B). *MEPCE* mRNA levels showed no significant decline during megakaryocytic differentiation, suggesting regulation of this factor at the protein level (Figure S1C).

Similar studies were carried out on a nontransformed murine hematopoietic cell line, HPC7, which retains cytokine-responsive multilineage differentiation potential (Pinto do O et al., 1998). These cells underwent rapid and efficient erythroid or megakaryocytic differentiation in response to 48 hr treatment with erythropoietin (Ery) or thrombopoietin (Mk), respectively (Figure S1D). As with primary human progenitors, HPC7 megakaryocytic differentiation specifically correlated with downregulation of the 7SK snRNP core components and upregulation of HEXIM1 (Figures 1D, 1E, and S1E). In addition, the HPC7 cells did not downregulate cyclin T1 or Cdk9 during megakaryocytic differentiation (Figure S1F). Glycerol gradient analysis of Cdk9 distribution between large, inactive and small, active complexes (Sedore et al., 2007) revealed 80% of megakaryocytic Cdk9 to be within the small complex (fraction 5). In erythroid and undifferentiated cells, by contrast, the majority of Cdk9 (~70%) resided in the large complex (fraction 9) (Figure 1F). (Fraction 3 contained insoluble debris and represents background.) Another validated approach toward assessment of intracellular P-TEFb status consists of immunoprecipitation to determine association with the repressor HEXIM1, an interaction dependent on the integrity of the 7SK snRNP core complex (Chen et al., 2008). This approach confirmed a decrease in cyclin T1-HEXIM1 complexes in HPC7 cells undergoing megakaryocytic differentiation, as compared with cells either undergoing erythroid differentiation (Figure 1G) or maintained undifferentiated (see Figure 2C). The results in Figure 1 thus suggest a lineage-specific mechanism of P-TEFb activation in megakaryopoiesis, during which the dissolution of the 7SK snRNP is accompanied by large-scale release of active P-TEFb.

Calpain Contribution to Megakaryocytic P-TEFb Activation and Differentiation

Mapping of the mammalian transcriptional protein interactome has identified calpain subunits (S1 and 2) as components of an extended 7SK snRNP network (Jeronimo et al., 2007), suggesting a role for proteolysis in remodeling of this complex. To examine the association of calpain with P-TEFb in a cell line model of megakaryocyte differentiation, K562 cells before and after phorbol ester (TPA) treatment underwent immunoprecipitation of endogenous cyclin T1 (CT1). As described for GATA1 (Elagib et al., 2008), calpain 2 displayed inducible recruitment to P-TEFb in association with differentiation induction (Figure 2A). By contrast, Cdk9 coprecipitated with cyclin T1 both before and after induction. Immunoprecipitation of endogenous HEXIM1 also revealed calpain 2 binding that was enhanced by TPA treatment, suggesting inducible recruitment of calpain 2 to the 7SK snRNP complex during megakaryocytic differentiation (Figure S2A).

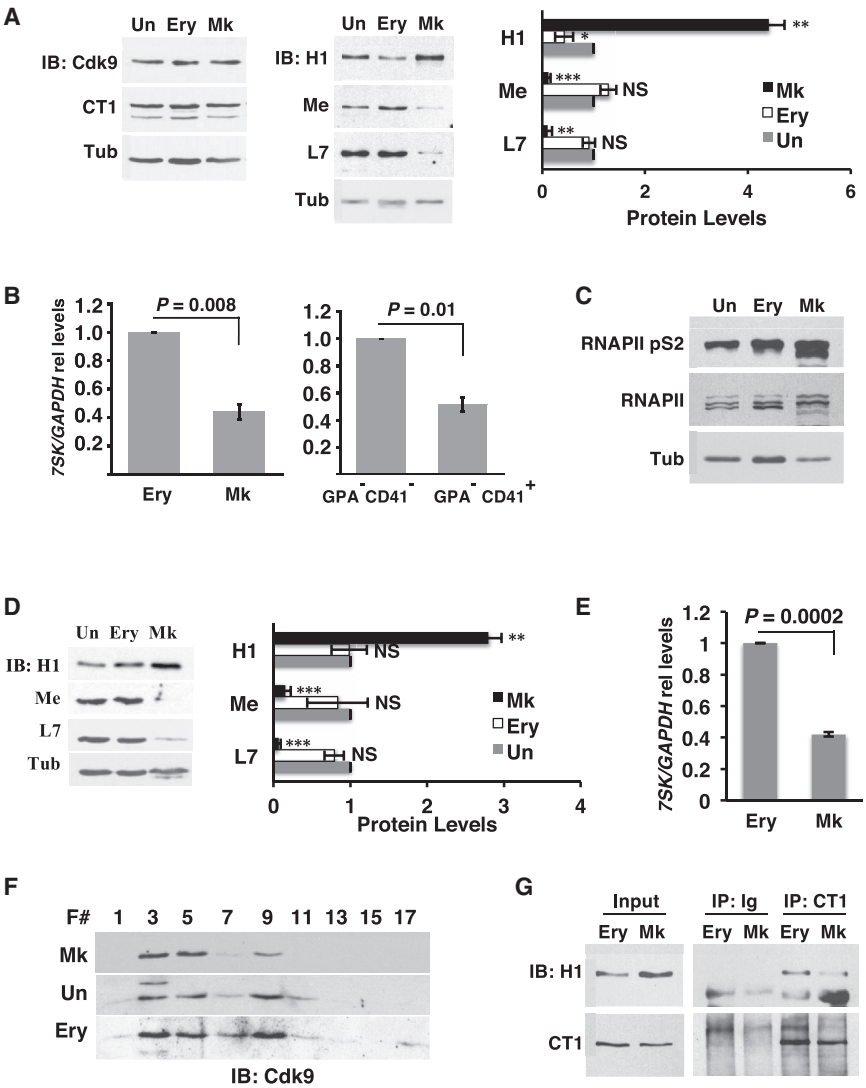

Figure 1. Megakaryocytic Downregulation of 7SK snRNP Core Components and Associated P-TEFb Release

(A) Analysis of 7SK snRNP protein components. (Left and middle panels) Primary human progenitors either undifferentiated (Un) or cultured for 5 days in erythroid (Ery) or megakaryocytic (Mk) medium underwent immunoblot for Cdk9, cyclin T1 (CT1), HEXIM1 (H1), MePCE (Me), LARP7 (L7), and tubulin (Tub). (Right panel) Scanning densitometry from three independent experiments conducted as in the middle panel. Results represent mean ± SEM for signals relative to those in undifferentiated cells. In addition, all signals are normalized to tubulin. *$p < 0.05$; **$p < 0.01$; ***$p < 0.005$; NS, not significant.

(B) (Left panel) Relative 7SK levels in human progenitors cultured as in (A). (Right panel) Relative 7SK levels in sorted CD41$^-$ GPA$^-$ double-negative and CD41$^+$ GPA$^-$ (Mk) cells from megakaryocytic culture. Graphs represent mean ± SEM of 7SK normalized to *GAPDH* in three independent experiments.

(C) Phosphorylation of RNA polymerase II carboxyl terminal domain serine 2 (RNAPII pS2). Human CD34+ progenitors cultured 3 days in expansion medium (Un) or 6 days in erythroid or megakaryocyte medium underwent immunoblotting of whole-cell lysates for RNAPII pS2, total RNAPII, or tubulin.

(D and E) HPC7 cells either undifferentiated (Un) or grown in Ery or Mk medium underwent analysis as in (A) and (B). Graphs both represent mean ± SEM for three independent experiments. ***$p < 0.005$.

(F and G) Megakaryocytic P-TEFb release. Extracts from HPC7 cells cultured as in (D) were subjected to glycerol gradient fractionation and immunoblotting for Cdk9 (F) or cyclin T1 immunoprecipitation followed by immunoblot for HEXIM1 (G). F #, fraction number.

See also Figure S1.

Evidence for lineage-selective, endogenous calpain activation was provided by immunoblot detection of a characteristic 190 kDa filamin A cleavage fragment (Xu et al., 2010), emerging during megakaryocytic, but not during erythroid differentiation of primary progenitors (Figure S2B). shRNA knockdowns confirmed that this cleavage depended on calpain 2 expression (see Figure 3E). Calpastatin, the endogenous calpain inhibitor with numerous isoforms (Takano et al., 1993; Wendt et al., 2004), showed strong erythroid upregulation of large (~110 kD) and small (~70 kD) variants with minimal megakaryocytic upregulation of a large variant; by contrast, calpain 2 showed megakaryocytic, but not erythroid, upregulation (Figure S2C). To assess the contribution of calpain activity to the megakaryocytic remodeling of the 7SK snRNP (see Figure 1), calpain protease inhibitors were added to primary megakaryocytic cultures. Notably, these inhibitors prevented both the downregulation of MePCE and the upregulation of HEXIM1 but had no effect on LARP7 (Figures 2B and S2D). In addition, short-term administration of the inhibitors prevented the dissociation of HEXIM1 from P-TEFb, as determined by coimmunoprecipitation analysis of HPC7 extracts (Figure 2C).

Participation of calpain in megakaryocytic differentiation was supported by the repressive effect of the inhibitors on cellular enlargement, polyploidization, and CD41 upregulation (Figures 2D and S2E). This finding raised the possibility that the block in MePCE downregulation associated with calpain inhibition might occur secondary to impaired megakaryocytic differentiation. To rule out this possibility, progenitors were allowed to undergo megakaryocytic differentiation and were subsequently treated for only 18 hr with calpain inhibitors. This short-course treatment reversed MePCE downregulation in the absence of any effects on megakaryocytic differentiation, consistent with a direct influence of calpain activity on MePCE levels (Figure S2D).

Multiple approaches were taken to confirm the contribution of calpain to megakaryocytic differentiation. Because calpain inhibitors also target cathepsin proteases, progenitors underwent control treatment with cathepsin inhibitors, which did not affect megakaryocytic differentiation (data not shown). In addition, we subjected progenitors to lentiviral shRNA knockdown of

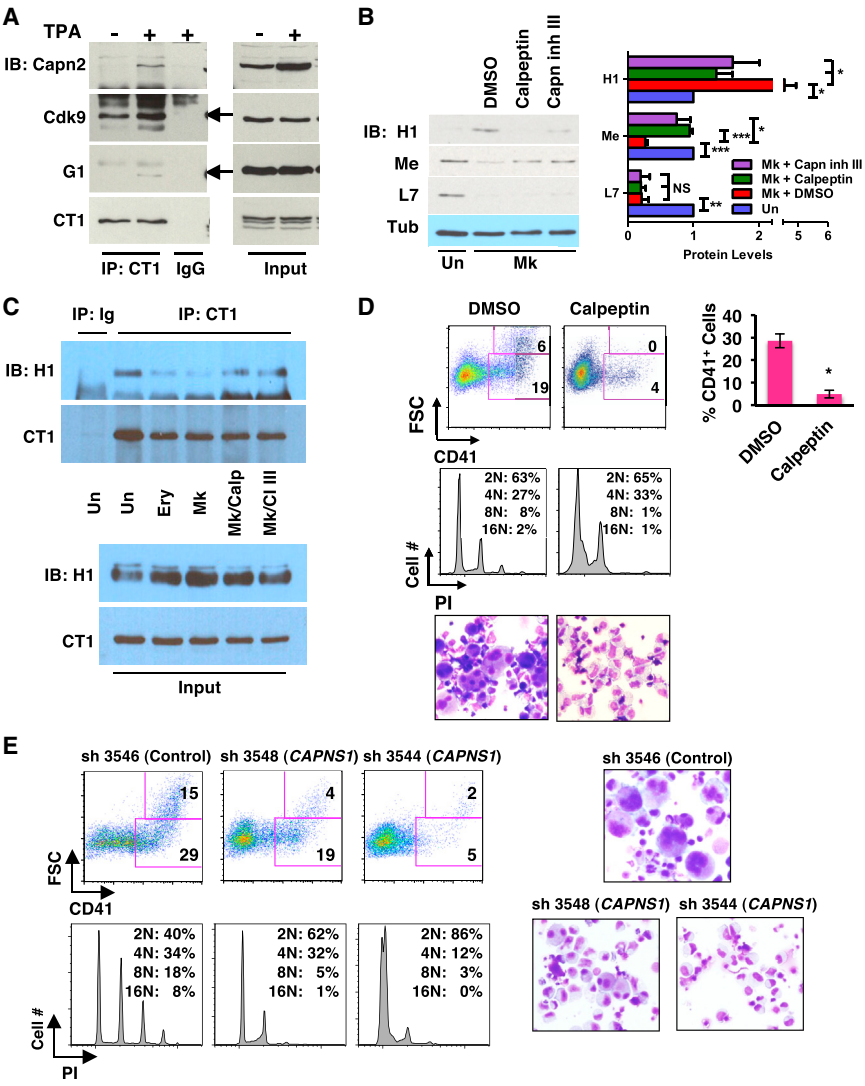

Figure 2. Calpain Contribution to Megakaryocytic P-TEFb Activation and Differentiation

(A) Analysis of calpain 2 association with P-TEFb. Extracts from K562 cells treated with either DMSO (–) or 25 nM TPA (+) underwent immunoprecipitation (IP) with antibody to cyclin T1 (CT1) or control immunoglobulin G followed by immunoblotting for calpain 2 (Capn2), Cdk9 (arrow), GATA-1 (G1) (arrow), and cyclin T1 (CT1).

(B) Effects of calpain inhibition on megakaryocytic MePCE downregulation and HEXIM1 upregulation. Primary human progenitors either undifferentiated (Un) or cultured in megakaryocytic medium (Mk) with DMSO, 40 μM calpeptin, or 20 μM calpain inhibitor III (Capn inh III) underwent immunoblot and densitometry as in Figure 1A. Results from three independent experiments are shown as mean ± SEM for signals relative to those in undifferentiated cells. In addition, all signals are normalized to tubulin. *p < 0.05; **p < 0.01; ***p < 0.005; NS, not significant.

(C) Effects of calpain inhibition on P-TEFb dissociation from HEXIM1. Extracts from HPC7 cells grown 48 hr in expansion (Un), erythroid (Ery), or megakaryocytic (Mk) medium underwent immunoprecipitation for cyclin T1 (CT1), followed by immunoblotting for HEXIM1 (H1) and CT1. The cells undergoing megakaryocytic culture were treated in the final 16 hr with either DMSO, 50 μM calpeptin (Calp), or 25 μM Capn inh III (CI III).

(D) Effects of calpain inhibition on megakaryocytic differentiation. Primary human progenitors grown for 6 days in megakaryocytic medium with DMSO or 40 μM calpeptin were analyzed by flow cytometry for CD41 expression and DNA content by propidium iodide staining (PI). Cell morphology was assessed by light microscopy of Wright-stained cytospins (200X). Graph represents mean ± SEM for CD41 expression in three independent experiments; *p < 0.05.

(E) Role of calpain S1 in megakaryocytic differentiation. Primary human progenitors transduced with lentiviral shRNA constructs targeting Calpain S1 (*CAPNS1*) underwent megakaryocytic culture for 5 days followed by analysis as in (C). For documentation of knockdown, see Figure S2E.

See also Figure S2.

calpain S1, the regulatory subunit required for calpain activity. Two different shRNAs diminished calpain S1 levels by ~3-fold (Figure S2F), and both blocked megakaryocytic differentiation in a manner similar to the calpain inhibitors (Figure 2E). The block in megakaryopoiesis caused by calpain inhibition was not associated with major impairments in viability or with redirection of cells down the erythroid lineage (data not shown).

To further validate calpain involvement in megakaryopoiesis, in vivo gene deletion was conducted by crossing *CAPNS1*$^{f/f}$ (S1$^{f/f}$) mice (Tan et al., 2006) with a deleter strain expressing Cre recombinase driven by the megakaryoctyic PF4 promoter (Tiedt et al., 2007). Despite evidence for incomplete excision in marrow megakaryocytic cultures (data not shown), *CAPNS1*$^{f/f}$;PF4-Cre (S1$^{f/f}$;PF4-Cre) mice had significant thrombocytopenia accompanied by normal red and white cell counts (Figure S2G). In addition, *CAPNS1*$^{f/f}$;PF4-Cre marrows showed defective megakaryocytic maturation in ex vivo cultures, reflected by impairments in upregulation of CD41/CD42 and in morphogenesis (Figure S2H; data not shown).

Implication of Calpain 2 as the Isozyme Mediating Megakaryopoietic P-TEFb Activation

The principal hematopoietic calpains that depend on calpain S1 for their activity consist of calpain 1 and calpain 2. To determine which of these isozymes might participate in regulating megakaryopoiesis, each underwent targeting by shRNAs in primary human progenitors, with ~2-fold isozyme-specific knockdowns obtained for both (Figure 3A). The calpain 2 knockdowns significantly impaired megakaryopoiesis, including CD41 upregulation, polyploidization, and cellular enlargement, whereas calpain 1 knockdowns had no effects distinct from those of transducing control vector (Figures 3B–3D). In addition, calpain 2, and not calpain 1, contributed to the filamin A cleavage observed during megakaryopoiesis (Figure 3E). shRNA knockdowns in K562

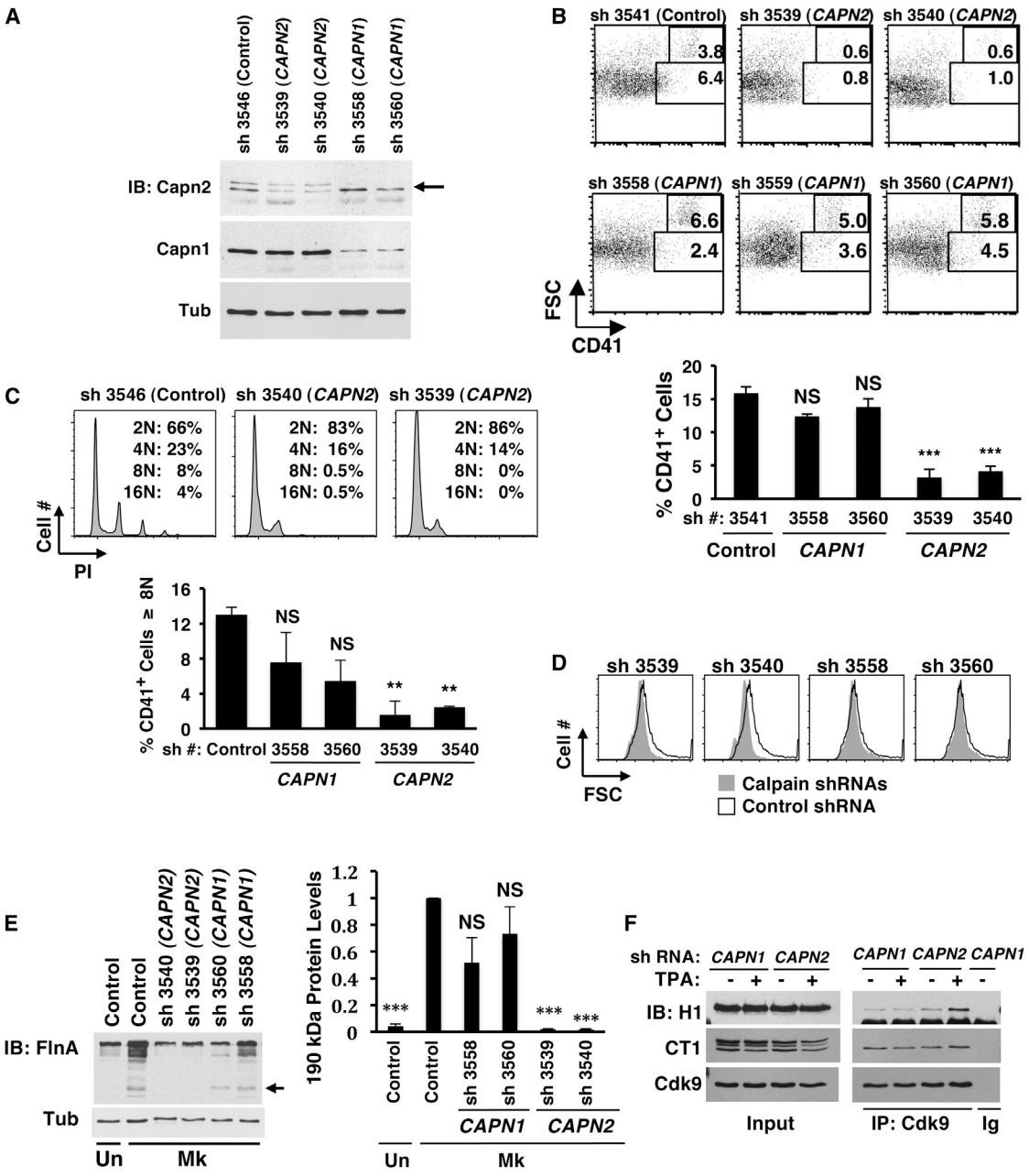

Figure 3. Implication of Calpain 2 as the Isoenzyme Involved in Megakaryocytic Differentiation

(A) Specificity of calpain 1 and 2 knockdowns. Primary human progenitors transduced with lentiviral shRNA constructs targeting calpain 1 (*CAPN1*) or 2 (*CAPN2*) were analyzed by immunoblot. Arrow: calpain 2; band above arrow: lot-dependent cross-reactivity of antibody to calpain 1; smear below arrow: most likely autolyzed calpain 2.

(B and C) Relative contributions of calpain 1 versus 2 to megakaryocytic differentiation. Progenitors transduced with lentiviral shRNA constructs as in (A) were analyzed for megakaryocytic differentiation as in Figure 2E. Graphs represent mean ± SEM for CD41 expression or for percentage of $CD41^+$ cells with DNA content of ≥8N, with both graphs derived from three independent experiments; $^{**}p < 0.01$; $^{***}p < 0.005$; NS, not significant.

(D) Relative contributions of calpain 1 versus 2 to cellular enlargement during megakaryopoiesis. Forward scatter (FSC) profiles of cells subjected to shRNA knockdowns and culture as in (B).

(E) Relative contributions of calpain 1 versus 2 to filamin A cleavage associated with megakaryocytic differentiation. (Left panel) Human progenitors transduced with shRNA constructs as (A) underwent megakaryocytic culture followed by immunoblotting for filamin A (FlnA). Arrow indicates 190 kDa cleavage fragment. (Right panel) Densitometric analysis of 190 kDa cleavage fragment from three independent experiments performed as in the left panel. Graph represents mean ± SEM; $^{***}p < 0.005$.

(F) Relative contributions of calpain 1 versus 2 to HEXIM1 dissociation from P-TEFb. K562 cells expressing shRNAs knocking down either calpain 1 or calpain 2 underwent induction with TPA (25 nM, 48 hr) followed by immunoprecipitation of Cdk9 and immunoblotting for HEXIM1 (H1), cyclin T1 (CT1), and Cdk9.

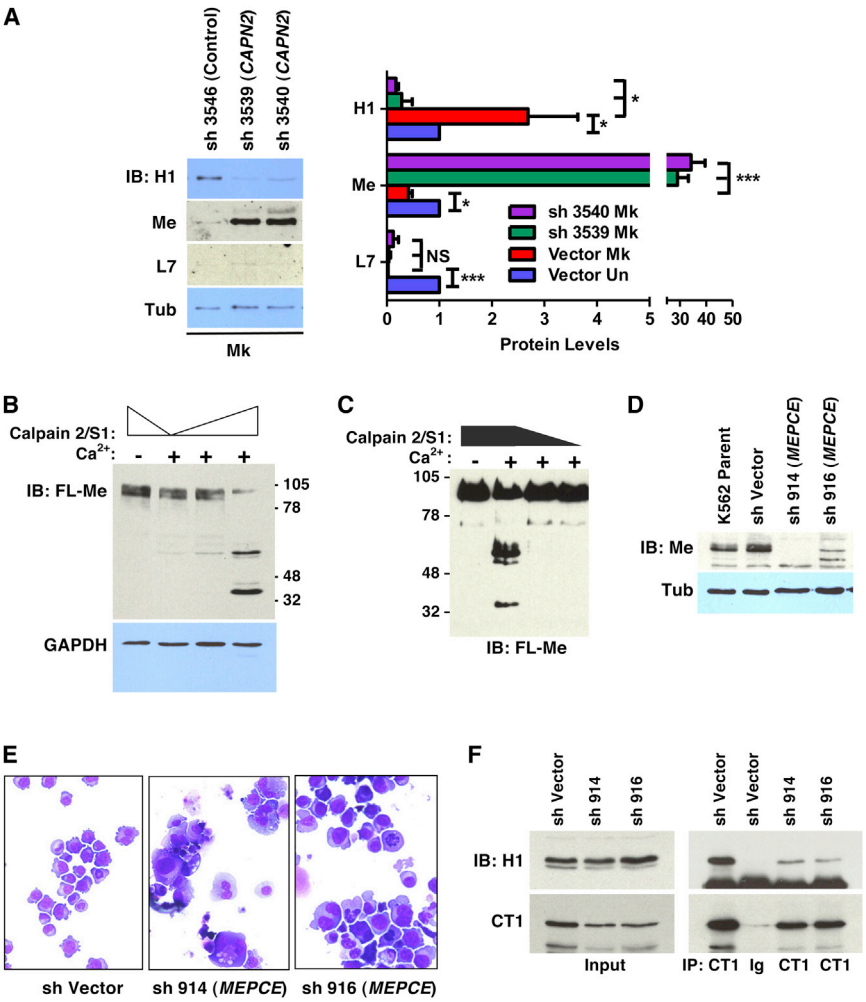

Figure 4. Involvement of Calpain 2 in Megakaryocytic Downregulation of MePCE and Consequences of MePCE Downregulation

(A) Effects of calpain 2 knockdown on MePCE (Me), HEXIM1 (H1), and LARP7 (L7) levels. Cells transduced and cultured as in Figure 3B underwent immunoblotting followed by scanning densitometry. Graph depicts mean ± SEM for three independent experiments. *$p < 0.05$; **$p < 0.01$; ***$p < 0.005$; NS, not significant.

(B) In vitro analysis of MePCE cleavage by calpain 2. Extracts from HEK293T cells transfected with FLAG-MePCE (FL-Me) expression vector were incubated with 50 to 200 ng purified calpain 2/S1 ± 2 mM $CaCl_2$ (Ca^{2+}), followed by immunoblot for FL-Me and GAPDH.

(C) In vitro analysis of MePCE cleavage by calpain 2. Purified FL-Me protein from HEK293T transfectants was subjected to in vitro cleavage and immunoblot as in (B).

(D and E) K562 cells transduced with shRNA constructs targeting MePCE underwent immunoblotting in (D). Cell morphology was assessed by light microscopy on Wright-stained cytospins (200X) in (E).

(F) Effect of MePCE downregulation on P-TEFb interaction with HEXIM1. Extracts from K562 cells subjected to shRNA knockdown of MePCE underwent immunoprecipitation of cyclin T1 followed by immunoblotting for HEXIM1 (H1) and cyclin T1 (CT1).

See also Figure S3.

cells ± TPA were conducted to compare contributions of calpain 1 versus calpain 2 to the dissociation of HEXIM1 from P-TEFb; knockdown of calpain 2 notably enhanced HEXIM1 association with P-TEFb, particularly in TPA treated cells (Figure 3F). As a leukemic cell line, K562 cells undergo incomplete megakaryocytic differentiation with TPA induction and, unlike nontransformed cells, lack dynamic regulation of HEXIM1 expression.

Calpain 2 involvement in megakaryopoietic P-TEFb activation was supported by a consistent decrease in HEXIM1 expression associated with its knockdown (Figures 4A and S3A), but not with calpain 1 knockdown (data not shown). In addition, MePCE showed dramatic upregulation in cells subjected to calpain 2 knockdown (Figures 4A and S3A), suggestive of direct proteolytic targeting. This notion was further supported by cell-free assays in which recombinant calpain 2/S1 cleaved MePCE in a calcium-dependent manner (Figures 4B and 4C). In these assays, calpain cleavage of MePCE in cellular extracts occurred with similar efficiency with or without RNase A addition, and MePCE isolated in complex with cyclin T1 underwent efficient digestion by calpain 2/S1 (Figures S3B and S3C). These findings suggest that calpain cleavage of MePCE may occur in the context of the 7SK snRNP complex. By contrast, calpain 2 knockdown failed to reverse megakaryocytic repression of LARP7 (Figures 4A and S3A), as observed with calpain inhibitors (see Figure 2B), consistent with a distinct, calpain-independent mechanism regulating this component of the 7SK snRNP. These results thus provide evidence for a developmental pathway in which calpain 2-dependent destruction of MePCE contributes, along with LARP7 downregulation, to ongoing P-TEFb activation, which in turn promotes megakaryocyte differentiation. Additional support for this pathway came from shRNA-mediated MePCE knockdown, which induced megakaryocyte morphogenesis in K562 cells and promoted dissociation of HEXIM1 from P-TEFb (Figures 4D–4F).

Calpain 2 and P-TEFb Regulation of Megakaryocytic Cytoskeleton Remodeling Factors

To characterize downstream factors regulated by calpain-P-TEFb signaling during megakaryopoiesis, in silico analysis was applied to identify genes whose expression covaried with *HEXIM1* during megakaryocytic differentiation (see Supplemental Experimental Procedures). *HEXIM1* was selected as the prototype based on its documented control by P-TEFb (Garriga et al., 2010; He et al., 2006) (see Figure S1B) and its calpain-dependent upregulation during megakaryopoiesis (see Figure 2B). Analysis of a data set derived from purified megakaryocytic progenitors at four distinct stages of development (Chen et al., 2007) revealed a group of four actin-associated cytoskeleton remodeling factors whose mRNA levels paralleled that of

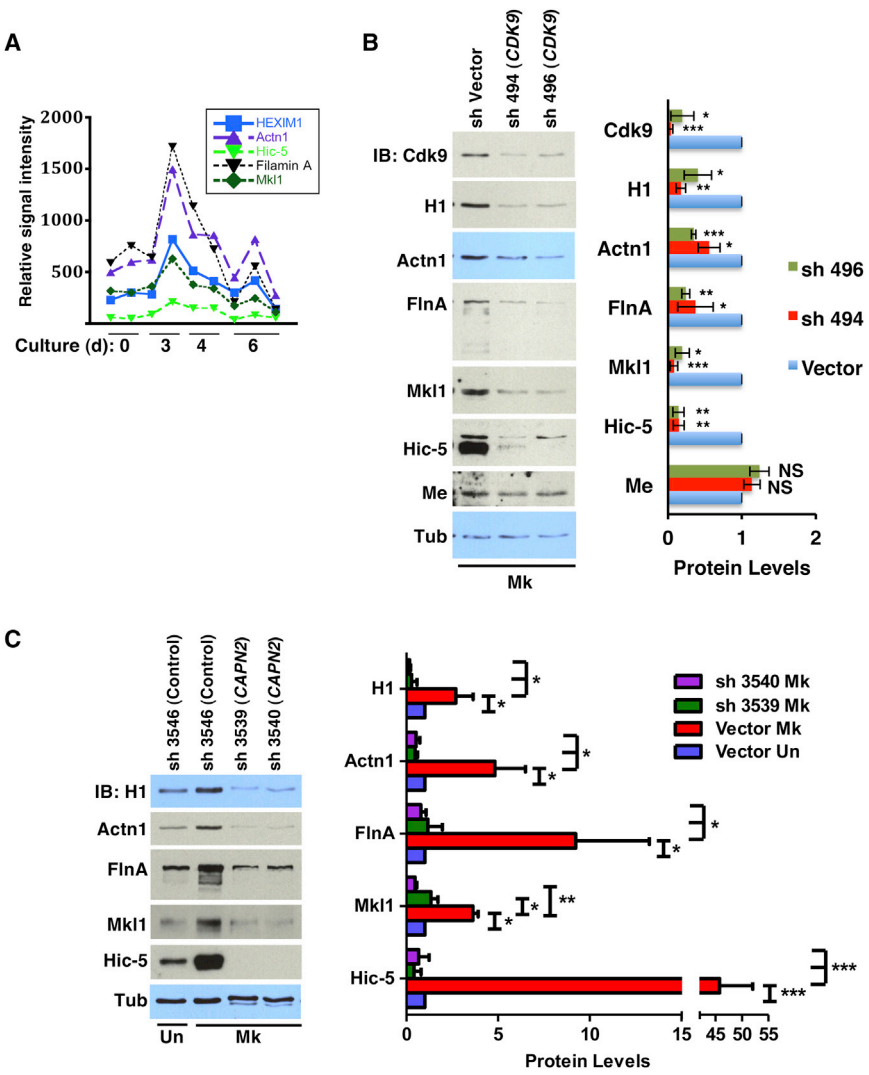

Figure 5. P-TEFb and Calpain 2 Regulate a Cohort of Megakaryocytic Cytoskeletal Remodeling Factors

(A) Expression patterns of gene cohort and *HEXIM1* during megakaryocytic differentiation. Normalized signals obtained from the GEO data set record GDS2521 comparing relative mRNA levels from murine fetal liver megakaryocytic progenitors at various developmental stages are plotted.

(B) Assessment of P-TEFb influence on expression of factors identified in (A). (Left panel) Primary human progenitors transduced with shRNA constructs targeting Cdk9 were cultured in megakaryocytic medium followed by immunoblot with the indicated antibodies. (Right panel) Densitometry derived from three independent experiments conducted as in the left panel showing mean ± SEM for relative protein levels normalized to Tubulin. *$p < 0.05$; **$p < 0.01$; ***$p < 0.005$; NS, not significant. HEXIM1 (H1), α-actinin 1 (Actn1), filamin A (FlnA), MePCE (Me), tubulin (Tub).

(C) Assessment of calpain 2 influence on expression of factors identified in (A). Progenitors subjected to calpain 2 knockdown were analyzed as in (B). Right: densitometry derived from three independent experiments conducted as in the left panel showing mean ± SEM for relative protein levels normalized to Tubulin. *$p < 0.05$; **$p < 0.01$; ***$p < 0.005$.

See also Figure S4.

HEXIM1 during megakaryopoiesis (Figure 5A). These factors, like HEXIM1, all displayed upregulation during megakaryocytic, but not erythroid, differentiation of primary progenitors (Figures S4A and S4B). Their regulation by P-TEFb was confirmed by Cdk9 knockdown in primary megakaryocytic cultures. Notably, the levels of all four factors, as well as of HEXIM1, decreased with knockdown of Cdk9, whereas the levels of MePCE and tubulin remained largely unaffected (Figure 5B). Cdk9 knockdown in undifferentiated cells did affect expression of these factors but not to the same extent as in the megakaryocytic knockdown (Figure S4C). Thus, Cdk9 likely plays a more prominent role in megakaryocytic upregulation of these factors than in their basal expression. Note that the relatively high Hic-5 expression seen in undifferentiated cells subjected to lentiviral transduction (Figure S4C), versus that in untransduced cells (Figure S4A), results from the extended culture period required for transduction and selection. Calpain 2 regulation of these cytoskeletal remodeling factors in megakaryocytes was also demonstrated by shRNA knockdowns in primary human progenitors (Figure 5C).

Two of the four factors, Mkl1 and filamin A, have been previously implicated in megakaryocyte development, including polyploidization (Begonja et al., 2011; Cheng et al., 2009). One of the factors, α-actinin, has been shown to regulate cytokinesis both in yeast and in mammalian cells (Mukhina et al., 2007; Wu et al., 2001). Notably, overexpression of α-actinin consistently causes a failure in cytokinesis, leading to polyploidization. As megakaryocytic endomitosis arises from a failure in cytokinesis (Lordier et al., 2008), we examined the contribution of α-actinin upregulation to megakaryocyte polyploidization and enlargement. Knockdown of α-actinin 1 in primary progenitors did not affect levels of HEXIM1 or Hic-5 but did diminish levels of filamin A, without affecting its proteolytic cleavage (Figure 6A). α-actinin thus does not exert feedback regulation of P-TEFb or calpain but may interact with filamin A. Phenotypically, α-actinin 1 knockdown prevented megakaryocytic polyploidization and enlargement but minimally affected CD41 upregulation (Figures 6B–6D and S5A; see Figures S5B–S5E for results with additional shRNA construct). These results therefore implicate α-actinin 1 as an important target downstream of calpain-P-TEFb signaling in megakaryocytic morphogenesis.

Calpain 2 Dysregulation in Association with the GATA1s Mutation

In genetic complementation studies comparing effects of introducing wild-type versus mutant GATA1 alleles into GATA1-deficient megakaryocytes, calpain 2 was previously identified as a GATA1 target gene with a distinct pattern of regulation.

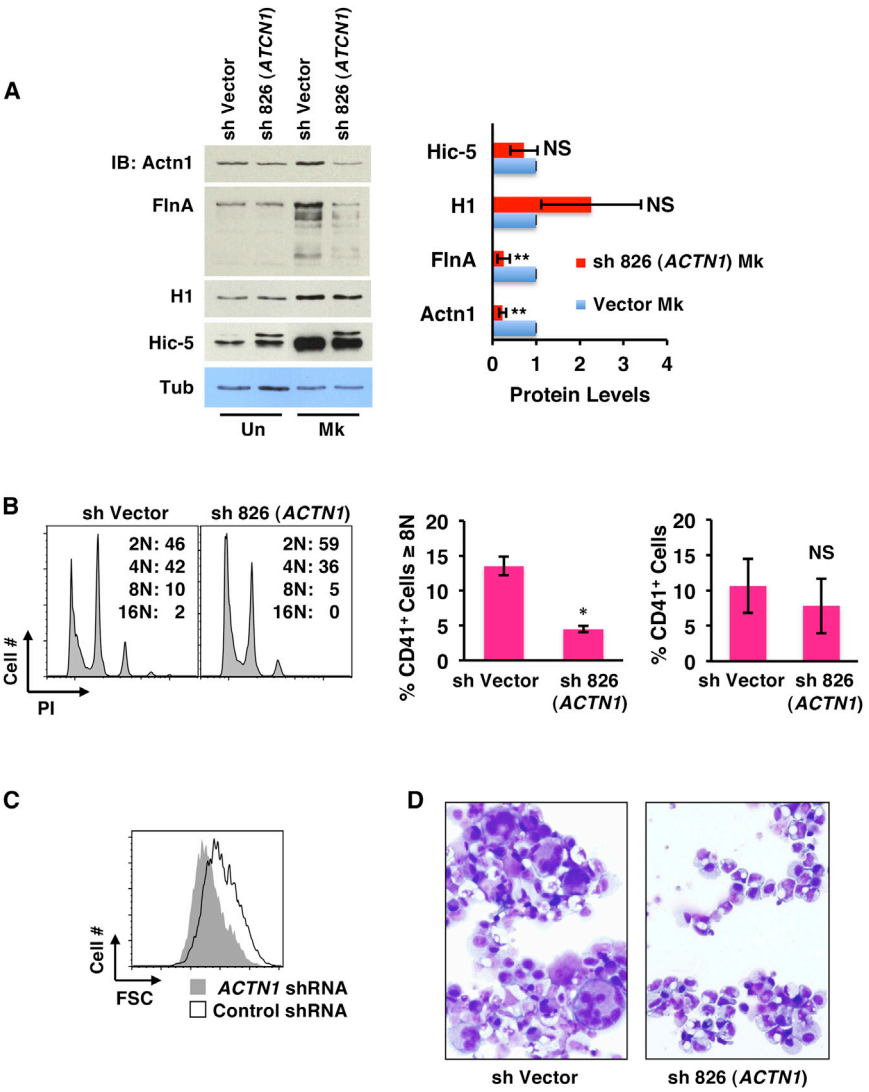

Figure 6. Contribution of α-Actinin-1 to Megakaryocytic Enlargement and Polyploidization

(A) Effects of megakaryocytic knockdown of α-actinin-1 on filamin A and Hic-5 expression. Primary human progenitors transduced with shRNA targeting α-actinin-1 (*ACTN1*) were analyzed as in Figure 5B. (Right panel) Densitometry derived from three independent experiments conducted as in the left panel showing mean ± SEM for relative protein levels normalized to Tubulin. *$p < 0.05$; **$p < 0.01$; NS, not significant. HEXIM1 (H1), α-actinin 1 (Actn1), filamin A (FlnA), tubulin (Tub).

(B–D) Effects of α-actinin-1 knockdown on megakaryocyte morphogenesis. Progenitors transduced with shRNA targeting α-actinin-1 underwent megakaryocytic culture followed by flow cytometry analysis as in Figures 3B–3D. Cell morphology was assessed by light microscopy of Wright-stained cytospins (200X). Graphs in (B) show mean ± SEM for three independent experiments. *$p < 0.05$; NS, not significant.

See also Figure S5.

Specifically, calpain 2 showed strong induction by wild-type GATA1 but poor induction by GATA1s, whereas most other GATA1 target genes studied showed equivalent regulation by both alleles (Muntean and Crispino, 2005). These findings suggested that the GATA1s mutation may interfere with calpain 2 upregulation during megakaryopoiesis. Independent support for this notion came from our analysis of the gene expression data set of Li et al. (2005) (GEO GDS1316), comparing fetal liver megakaryocytes from wild-type versus GATA1s knockin mice (G1s Ki). This data set clearly confirmed an association between the GATA1s mutation and defective megakaryocytic upregulation of calpain 2, with no abnormalities seen in calpain 1 expression (Figures 7A and S6A). Megakaryocytes deficient in overall GATA1 expression, from the G1 Lo strain, also showed markedly diminished calpain 2 expression. To assess potential consequences of the calpain 2 deficiency in G1s Ki megakaryocytes, this data set was further analyzed for expression patterns of the calpain 2-regulated cytoskeletal remodeling factors (see Figure 5C). Notably, all four factors showed profiles nearly identical to that of calpain 2, including defective upregulation in G1s Ki and G1 Lo megakaryocytes (Figure S6B). Thus, the calpain 2 deficiency associated with GATA1s may impair the developmental induction of key morphogenetic mediators.

To determine whether calpain 2 deficiency also correlated with the GATA1s mutation in patient samples, we analyzed the gene expression data set of Bourquin et al. (2006) (GEO GSE4119) comparing Down syndrome-associated (DS) versus non-Down syndrome-associated (non-DS) megakaryoblastic neoplasms. In this data set, the GATA1s mutation occurred in all DS cases and in none of the non-DS cases. Notably, the DS acute megakaryoblastic leukemia (DS-AMKL) cases expressed significantly less calpain 2 than did non-DS AMKL cases (Figure 7B). Because of clinical and molecular heterogeneity within AMKL, we also compared two well-defined infantile megakaryoblastic neoplasms: DS transient myeloproliferative disorder (DS-TMD) versus AMKL with the t(1;22) chromosomal abnormality. Again, significantly less calpain 2 expression occurred in the DS samples (Figure S6C), confirming a clinical correlation between the GATA1s mutation and calpain 2 deficiency. TP53BP2, a control gene neighboring calpain 2 on chromosome 1, showed no differences in expression between the DS-TMD versus t(1;22) cases (data not shown).

Contribution of Calpain 2 Deficiency to GATA1s-Associated Dysmegakaryopoiesis

The GATA1s mutation causes abnormalities in fetal liver megakaryopoiesis, including excessive cellular proliferation and impaired upregulation of several differentiation markers (Li et al., 2005). Consistent with these prior findings, we observed defects in CD42 upregulation, polyploidization, and cellular enlargement

in G1s Ki fetal liver megakaryocytes (Figures 7C and 7D, compare wild-type [WT] vector versus G1s Ki vector; Figure S6E). Immunoblot analysis confirmed diminished calpain 2 protein expression in G1s Ki megakaryocytes, with no alteration in calpastatin levels (Figure S6D). Consistent with its regulation of P-TEFb activity, calpain 2 deficiency in G1s Ki megakaryocytes correlated with global deficiency in phosphorylation on serine 2 within the carboxy terminal domain of RNA polymerase II (Figure S6D). To determine whether calpain 2 deficiency contributes to GATA1s-associated dysmegakaryopoiesis, fetal liver cells transduced with control or calpain 2-expressing lentivirus underwent megakaryocytic culture and analysis. Transduction of G1s Ki cells with calpain 2-expressing lentivirus significantly enhanced several differentiation parameters within the $CD41^+$ megakaryocytic population: CD42 expression, polyploidization, proliferation arrest reflected by PKH26 dye retention, and cellular enlargement (Figures 7C and 7D). By comparison, nontransduced (GFP^-) megakaryocytic cells derived from control vector versus calpain 2 lentiviral exposures showed no differences in these parameters (data not shown). Wild-type fetal liver megakaryocytes transduced with calpain 2 lentivirus also showed increases in CD42 expression, cellular enlargement, and polyploidization (see Figures 7C and 7D). However, the impact of enforcing calpain 2 expression in wild-type cells was significantly less than in G1s Ki cells (see graphs in Figures 7C and 7D). With regard to proliferation, enforced calpain 2 had no significant effect in wild-type cells, in contrast to its arresting effect in G1s Ki cells (Figure 7C). A protease-deficient calpain 2 mutant (C105S) completely failed to rescue cellular enlargement in G1s Ki fetal liver progenitors and relatively weakly augmented CD42 levels, the latter effect possibly due to calpastatin sequestration (Figures S6F and S6G). To determine whether MePCE downregulation might contribute to the rescue conferred by enforced calpain 2 expression, G1s Ki fetal liver cells underwent shRNA-mediated MePCE knockdown, which enhanced cellular enlargement and CD42 expression (Figure 7F). In aggregate, these results support calpain 2 deficiency and consequent failure of MePCE downregulation as factors contributing to the defective fetal megakaryopoiesis associated with the GATA1s mutation (see pathway diagram in Figure 8).

DISCUSSION

The hypertrophic response in cardiomyocytes is driven by P-TEFb activation through a mechanism involving dissociation of Cdk9-Cyclin T complexes from the 7SK snRNP (Sano et al., 2002). How hypertrophic signaling induces this dissociation remains unclear but may involve a conformational shift in the 7SK snRNP complex elicited by the phosphatase activity of calcineurin (Chen et al., 2008). Recent studies have revealed a contribution of calpain activity to cardiomyocyte hypertrophy in diabetic mice, and calpain activation also maintains cardiomyocyte integrity during hemodynamic stress (Li et al., 2011; Taneike et al., 2011). This latter function appears to occur through a membrane repair mechanism but may also involve coordinated programming of cytoskeletal remodeling (Yamaguchi et al., 2012).

In megakaryopoiesis, the morphogenetic program appears to be initiated by calpain 2-mediated proteolysis of MePCE, a critical 7SK snRNP core component known to stabilize the 7SK snRNA (Barboric et al., 2009; Xue et al., 2010). Megakaryocytic calpain activation correlates with upregulation of calpain 2 but must also involve specialized signaling via calcium influx, upon which calpain function is absolutely dependent (Campbell and Davies, 2012). An additional contribution to differential calpain activation in megakaryocytic versus erythroid cells likely resides in the erythroid-specific upregulation of calpastatin, that is, the calpain inhibitor (Figure S2C). During megakaryopoiesis, calpain-induced downregulation of the 7SK snRNA, a required cofactor for HEXIM repression of Cdk9 (Michels et al., 2004; Yik et al., 2003), uncouples P-TEFb from repressive feedback mediated by continually rising HEXIM1 levels. In addition to calpain-dependent downregulation of MePCE, a distinct mechanism involving calpain-independent downregulation of LARP7, another 7SK snRNP core component, probably contributes as well to megakaryocytic downregulation of 7SK snRNA. Mechanisms for LARP7 downregulation could potentially involve alternative proteolytic pathways as well as transcriptional and posttranscriptional repression. Thus, multiple pathways during megakaryopoiesis likely cooperate in promoting global and irreversible shifting of P-TEFb toward its active form, thereby driving progression along a developmental pathway of continual cellular enlargement (see Figure 8). Whether megakaryocytic P-TEFb activation reinforces the very pathways that promote its activation is an intriguing topic for future investigation.

Normal megakaryopoiesis comprises, among many changes, the coordinated upregulation of cytoskeletal regulatory proteins that promote the dramatic cellular enlargement. Comparisons of transcriptional profiles from discrete developmental stages of megakaryopoiesis show activation of cytoskeletal-associated genes to occur early, concomitant with activation of genes in the m-calpain (calpain 2) pathway (Chen et al., 2007). Similarly, analysis of genes upregulated during polyploidization has identified a large cohort of cytoskeletal factors, including *ACTN1* (encoding α-actinin-1) (Raslova et al., 2007). Factors previously known to contribute to megakaryocytic cytoskeletal remodeling include SRF and Mkl1 (also known as MAL or MRTF-A), which together transactivate genes contributing to actin stress-fiber formation (Gilles et al., 2009; Halene et al., 2010).

In the current study, four cytoskeletal regulatory factors were found to be controlled by the calpain 2-P-TEFb signaling pathway. One of these factors, Mkl1, itself regulates expression of cytoskeletal genes during megakaryopoiesis. Three of the factors, α-actinin, Hic-5, and Mkl1, have been implicated in cardiomyocyte hypertrophy (Kuwahara et al., 2010; Ridinger et al., 2009; Yund et al., 2009). Two of the factors, α-actinin and filamin A, function in actin crosslinkage, leading to F-actin stabilization (Mukhina et al., 2007; Nakamura et al., 2011), and our data suggest that α-actinin may regulate filamin A levels in megakaryocytes (Figure 6A). An interesting property shared by Mkl1, Hic-5, and filamin A consists of their dual functions as actin-binding factors in the cytosol and transcriptional regulators in the nucleus (Gilles et al., 2009; Heitzer and DeFranco, 2006; Nakamura et al., 2011), potentially allowing for cytoskeletal-nuclear crosstalk during megakaryopoiesis. Studies of megakaryopoiesis in knockout mice have demonstrated participation of both Mkl1 and filamin A in polyploidization (Begonja et al., 2011; Cheng et al., 2009). Our knockdown experiments in primary

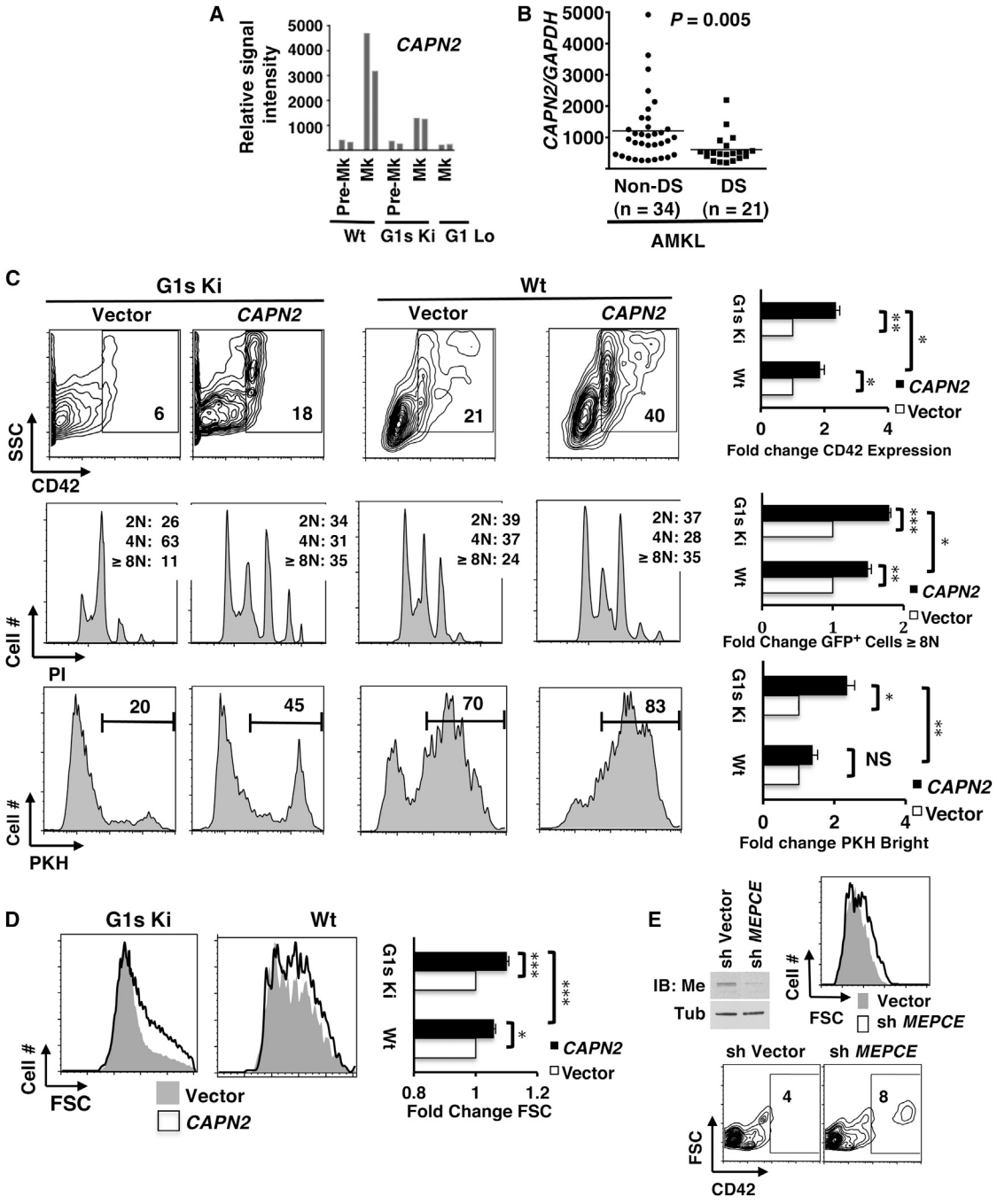

Figure 7. Calpain 2 Deficiency Occurs in Megakaryocytic Cells with Mutant GATA1s and Contributes to Aberrant Megakaryopoiesis

(A) Expression patterns of calpain 2 (*CAPN2*) in developing fetal liver megakaryocytes from wild-type (WT), GATA1s knockin (G1s Ki), and megakaryocytic GATA1 knockout (G1 Lo) mice. Normalized signals obtained from the GEO data set record GDS1316 comparing relative mRNA levels from murine fetal liver pre-megakaryocytes (pre-Mk) and megakaryocytes (Mk) of the indicated strains are plotted. Paired bars represent two independent experiments.

(B) Calpain 2 expression in human megakaryocytic proliferative disorders bearing the GATA1s mutation. Normalized signals obtained from the GEO data set record GSE4119 comparing relative mRNA levels from cases of acute megakaryoblastic leukemia occurring in patients with Down syndrome (DS-AMKL) versus cases unassociated with Down syndrome (non-DS-AMKL) are plotted.

(C and D) Effects of lentiviral-mediated calpain 2 restoration on megakaryocytic differentiation in fetal liver progenitors with GATA1s mutation. Day 13.5 fetal liver progenitors from G1s Ki and wild-type (WT) mice underwent transduction with calpain 2 or control lentiviral expression constructs, followed by megakaryocytic culture and flow cytometric analysis. GFP$^+$-transduced cells were analyzed for expression of CD42, ploidy (PI), megakaryocytic growth arrest (PKH26 retention in CD41$^+$ cells), and megakaryocytic cell size (FSC in CD41$^+$ cells). Each of the four graphs in (C) and (D) represent mean ± SEM for three independent experiments. Graphic results are presented as fold change relative to vector-transduced cells within each strain; *p < 0.05; **p < 0.01; ***p < 0.005; NS, not significant.

(legend continued on next page)

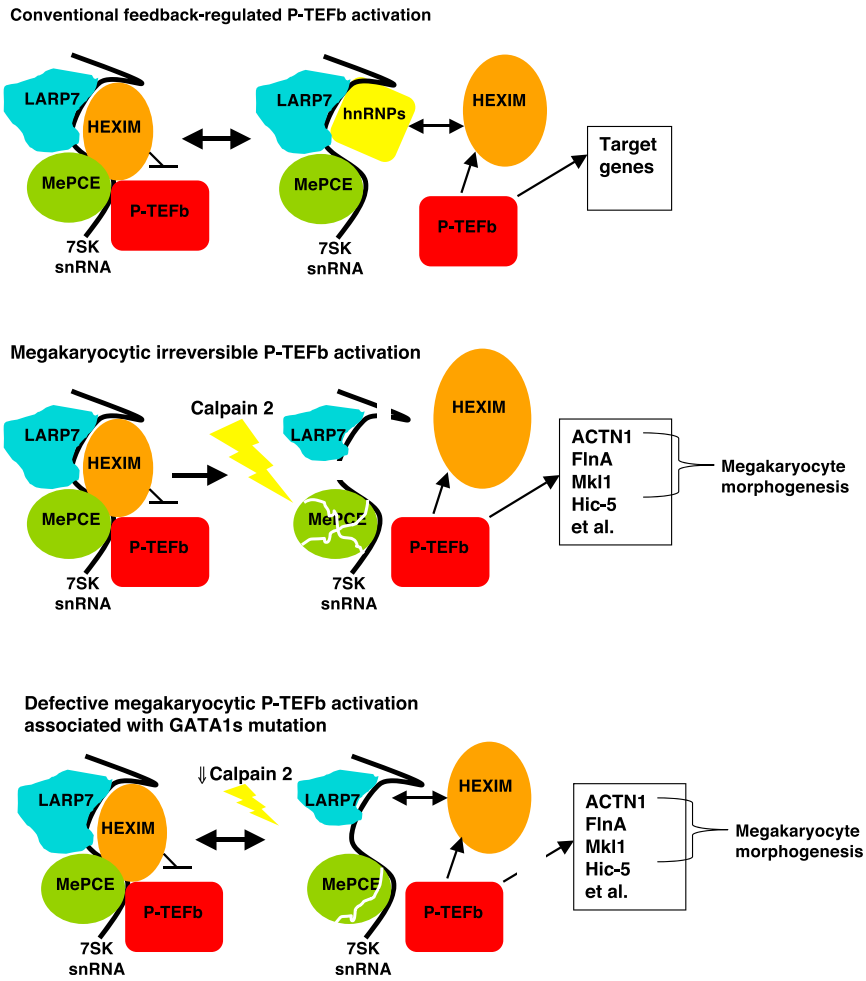

Figure 8. A Model Depicting the Pathway for P-TEFb Activation in Megakaryopoiesis and Perturbation of This Pathway by a Leukemogenic GATA1 Mutation

In the top panel, nonmegakaryocytic cells, such as erythroblasts, show reversible, feedback-regulated P-TEFb activation in which P-TEFb and HEXIM1 reversibly associate with the 7SK snRNP. In this scenario, the majority of P-TEFb resides within the large inactive complex.

In the middle panel, megakaryocytes show global and irreversible P-TEFb activation. In this scenario, calpain 2 undergoes upregulation and activation, promoting 7SK snRNP destruction through direct proteolysis of MePCE. An additional contribution derives from calpain-independent LARP7 downregulation. In the absence of the 7SK snRNP, chronic unopposed P-TEFb activation drives transcription of a cohort of genes that includes cytoskeletal remodeling factors that promote megakaryocyte morphogenesis and HEXIM1.

In the bottom panel, megakaryocytic upregulation of calpain 2 is impaired in cells bearing the leukemogenic GATA1s mutation. These cells show impairment in the destruction of the 7SK snRNP, retain capacity for feedback inhibition of P-TEFb, and are compromised in the activation of key P-TEFb target genes.

human progenitors identify α-actinin-1 as an additional factor whose upregulation contributes to megakaryocytic polyploidization and enlargement (Figures 6B–6D; Figures S5C–S5E). Future experiments will address whether Hic-5 contributes to megakaryocyte morphogenesis and the extent to which these cytoskeletal factors engage in crosstalk.

The leukemia-associated GATA1 mutant, GATA1s, causes developmental abnormalities, including hyperproliferation in fetal liver megakaryocytic progenitors (Li et al., 2005). The transcriptional defects in GATA1s responsible for these abnormalities have been attributed to a loss of repressive control over oncogenic factors such as c-Myc, c-Myb, PU.1, Ikaros, and GATA-2 and an array of E2F target genes (Klusmann et al., 2010; Li et al., 2005). The defects in GATA1s function may arise from loss of a binding domain for pRb and E2F (Kadri et al., 2009; Klusmann et al., 2010). Our data suggest that loss of an activation function, namely, upregulation of calpain 2, also represents a critical defect in GATA1s. Previous data show GATA1s to retain normal activation capability for most megakaryocytic target genes examined, with the exception of calpain 2 and GP1bα (Muntean and Crispino, 2005). The ability of enforced calpain 2 expression to induce CD42 upregulation in G1s Ki fetal liver megakaryocytes (Figure 7C) suggests that GP1bα may lie downstream of calpain 2 in GATA1 regulation of megakaryopoiesis. The likelihood that defective signaling via calpain 2 to P-TEFb contributes to DS megakaryocytic neoplasia is supported by the deficiency of calpain 2 expression in DS-AMKL/TMD specimens and by studies in which P-TEFb inhibition in mice elicits a megakaryoblastic disorder resembling DS-TMD (Elagib et al., 2008). Future studies will examine the interplay of pRb-E2F, Calpain 2-P-TEFb, and other hypertrophic pathways in normal and neoplastic megakaryopoiesis.

EXPERIMENTAL PROCEDURES

Cell Culture

Purified primary human CD34$^+$ hematopoietic progenitors were cultured in serum-free unilineage media as described previously (Elagib et al., 2008). Undifferentiated cells (Un) were cultured in prestimulation medium for 72 hr. Erythroid (Ery) and megakaryocytic (Mk) cells were cultured in their respective media for the indicated durations following an initial prestimulation phase. Protease inhibitors (EMD Chemicals) dissolved in DMSO or DMSO only were added to cultures as indicated. K562 and HEK293T cells were cultured under standard conditions (Elagib et al., 2008). HPC7 cells were maintained in growth

(E) Impact of MePCE knockdown on megakaryocyte differentiation in G1S Ki fetal liver cells. Embryonic day 13.5 fetal liver cells were transduced with lentiviral shRNA constructs, selected in puromycin, subjected to Mk culture, and analyzed for size (FSC) and CD42 upregulation. Immunoblot on left shows knockdown of MePCE in MEL cells transduced with the shRNA to MEPCE (A5).
See also Figure S6.

medium (IMDM, 5% FBS, 100 ng/ml SCF) as described previously (Pinto do O et al., 1998); for differentiation induction, the cells were cultured 48 hr in either megakaryocyte medium (IMDM, 5% FBS, 2.5 ng/ml SCF, 50 ng/ml TPO, 10 ng/ml IL-6) or erythroid medium (IMDM, 5% FBS, 20 ng/ml SCF, 4 U/ml EPO). Fetal liver cells from day 13.5 mouse embryos were dissaggregated, depleted of red cells, and then expanded in a 1:1 mixtue of RPMI 1640 and Dulbecco's modified Eagle's medium supplemented with 100 ng/ml SCF, 20 ng/ml IL-3, 2 U/ml erythropoietin, and 1% Nutridoma (Roche). To promote megakaryopoiesis, the cells were transferred to RPMI 1640 with 10% fetal bovine serum, 25 ng/ml SCF, and 10 ng/ml TPO. To prevent shedding of the CD42 antigen (Nishikii et al., 2008), the medium was supplemented after the initial 24 hr with 20 μM GM6001 (EMD Chemicals). Megakaryocytic cultures derived from marrow of 5-FU-treated mice were performed as described by Hamlett et al. (2008).

Cell Transduction and Transfection

For lentiviral shRNA-mediated knockdown, pLKO.1-derived constructs targeting human mRNAs of interest were purchased from Open Biosystems. For lentiviral expression of calpain 2, a full-length rat cDNA was inserted upstream of an IRES element previously introduced into pWPXLD, a parent vector provided by Didier Trono (École Polytechnique Fédéral de Lausanne). Construct packaging by HEK293T cotransfection with pCMV-dR8.74 plus pMD2.G was followed by spinoculation of target cells (Elagib et al., 2008). Cells transduced with shRNA constructs underwent selection with puromycin, 2 μg/ml during an initial 72 hr expansion phase and 1 μg/ml during the subsequent differentiation phase. FLAG-MePCE plasmid was a gift from Dr. Matjaz Barboric (University of Helsinki) (Barboric et al., 2009).

Immunoprecipitation, Immunoblot, and RNA Quantitation

Immunoprecipitation of endogenous P-TEFb and HEXIM1 from HPC7 and K562 cellular extracts, followed by immunoblot detection, was performed as described (Elagib et al., 2008). For direct immunoblot analysis of cells, whole-cell lysates in 1X SDS-PAGE loading buffer supplemented with protease and phosphatase inhibitors underwent shearing of DNA prior to standard analysis (Elagib et al., 2008). Densitometry data were acquired on a GS800 calibrated densitometer (Bio-Rad) and analyzed with Quantity One software (Bio-Rad). For quantitation of *HEXIM1*, *MEPCE*, and *7SK*, total cellular RNA isolated using the RNeasy Plus Mini Kit (QIAGEN) underwent conversion to cDNA using the iScript kit (Bio-Rad Life Science) followed by quantitative PCR on the iCycler platform using iQ SYBR Green Supermix (Bio-Rad). Relative transcript levels were calculated using *GAPDH* normalization with the $\Delta\Delta C_T$ formula.

Glycerol Gradient Analysis

HPC7 extracts (in 150 mM NaCl, 2 mM MgCl2, 10 mM HEPES, 1 mM DTT, 1 mM PMSF, 20 μM calpain inhibitor III, EDTA-free protease inhibitor cocktail [Roche], 40 U/ml RNase inhibitor [Promega], and 0.5% NP-40) were loaded on 10%–45% glycerol gradients prepared in extraction buffer. The gradients were spun in a SW-41 rotor at 40,000 g for 16 hr at 4°C, and resultant fractions underwent SDS-PAGE-immunoblot.

In Vitro MePCE Cleavage Assays

FLAG-MePCE purified from HEK293T transfectants, or unpurified extracts, underwent incubation in a 30 μl reaction volume with 50–200 ng His_6-Calpain 2/S1 complex purified from *Escherichia coli* (EMD Chemicals). Where indicated, $CaCl_2$ was added to a final concentration of 2 mM. After incubation at 30°C for 15 min, the reaction was stopped by addition of an equal volume of 2X SDS-PAGE loading buffer with 100 μM calpain inhibitor III, followed by immunoblot analysis with anti-FLAG and anti-MePCE antibodies.

Flow Cytometry and Cell Sorting

CD41 and GPA in human progenitors, CD41 in murine progenitors, and ploidy in both species were assessed as described (Elagib et al., 2008). For antibody detection of murine CD42b, cells were stained with phycoerythrin-conjugated anti-GPIbα (Emfret Analytics). Dye dilution analysis of proliferation was performed on fetal liver cells after spinoculation and involved washing of cells followed by incubation with the red membrane dye PKH26 (Sigma-Aldrich). After stopping the staining reaction with 1% BSA, cells underwent washing followed by culture for 72 hr in megakaryocytic medium. Proliferation of transduced megakaryocytes was analyzed by gating on GFP^+ $CD41^+$ cells. For cell sorting, progenitors costained for CD41 and GPA were fractionated on a FACSVantage SE. Turbo Sorter with DIVA Option (Becton Dickinson).

Mice

Mice with megakaryocytic deletion of Calpain S1 were derived from the *capn4*^{PZ} strain (Tan et al., 2006). The PF4-Cre transgenic strain was purchased as C57BL/6-Tg(Pf4-cre)Q3Rsko/J (The Jackson Laboratory). The G1S Ki mice consisted of the *GATA1*$^{\Delta E2}$ strain (Li et al., 2005). Blood obtained by retro-orbital phlebotomy was analyzed for complete blood count values (CBC) on a Hemavet 950FS analyzer (Drew Scientific).

Statistical Analysis

Statistical comparisons between two groups employed Student's t test (two-tailed, unpaired), and comparisons among >2 groups employed ANOVA.

SUPPLEMENTAL INFORMATION

Supplemental Information includes Supplemental Experimental Procedures and six figures and can be found with this article online at http://dx.doi.org/10.1016/j.devcel.2013.11.013.

ACKNOWLEDGMENTS

This paper is dedicated to the memory of Marcia Finberg. We thank Dr. Matjaz Barboric for the FLAG-MePCE expression construct, Dr. Leif Carlsson for HPC7 cells, Dr. Didier Trono for lentiviral plasmids, and Daniel Matson for generous assistance with glycerol gradient analysis. For helpful discussions and advice, we thank Drs. B. Matija Peterlin, David Price, Prabu Reddi, and Vijay Sankaran. This work was supported by grants from the National Institutes of Health (CA100057, DK079924, and DK090926).

Received: January 28, 2013
Revised: August 1, 2013
Accepted: November 18, 2013
Published: December 23, 2013

REFERENCES

Barboric, M., Lenasi, T., Chen, H., Johansen, E.B., Guo, S., and Peterlin, B.M. (2009). 7SK snRNP/P-TEFb couples transcription elongation with alternative splicing and is essential for vertebrate development. Proc. Natl. Acad. Sci. USA *106*, 7798–7803.

Bartholomeeusen, K., Xiang, Y., Fujinaga, K., and Peterlin, B.M. (2012). BET bromodomain inhibition activates transcription via a transient release of P-TEFb from 7SK snRNP. J. Biol. Chem. *287*, 36609–36616.

Begonja, A.J., Hoffmeister, K.M., Hartwig, J.H., and Falet, H. (2011). FlnA-null megakaryocytes prematurely release large and fragile platelets that circulate poorly. Blood *118*, 2285–2295.

Bottardi, S., Zmiri, F.A., Bourgoin, V., Ross, J., Mavoungou, L., and Milot, E. (2011). Ikaros interacts with P-TEFb and cooperates with GATA-1 to enhance transcription elongation. Nucleic Acids Res. *39*, 3505–3519.

Bourquin, J.-P., Subramanian, A., Langebrake, C., Reinhardt, D., Bernard, O., Ballerini, P., Baruchel, A., Cavé, H., Dastugue, N., Hasle, H., et al. (2006). Identification of distinct molecular phenotypes in acute megakaryoblastic leukemia by gene expression profiling. Proc. Natl. Acad. Sci. USA *103*, 3339–3344.

Campbell, R.L., and Davies, P.L. (2012). Structure-function relationships in calpains. Biochem. J. *447*, 335–351.

Chen, Z., Hu, M., and Shivdasani, R.A. (2007). Expression analysis of primary mouse megakaryocyte differentiation and its application in identifying stage-specific molecular markers and a novel transcriptional target of NF-E2. Blood *109*, 1451–1459.

Chen, R., Liu, M., Li, H., Xue, Y., Ramey, W.N., He, N., Ai, N., Luo, H., Zhu, Y., Zhou, N., and Zhou, Q. (2008). PP2B and PP1alpha cooperatively disrupt 7SK

snRNP to release P-TEFb for transcription in response to Ca2+ signaling. Genes Dev. *22*, 1356–1368.

Cheng, E.C., Luo, Q., Bruscia, E.M., Renda, M.J., Troy, J.A., Massaro, S.A., Tuck, D., Schulz, V., Mane, S.M., Berliner, N., et al. (2009). Role for MKL1 in megakaryocytic maturation. Blood *113*, 2826–2834.

Contreras, X., Barboric, M., Lenasi, T., and Peterlin, B.M. (2007). HMBA releases P-TEFb from HEXIM1 and 7SK snRNA via PI3K/Akt and activates HIV transcription. PLoS Pathog. *3*, 1459–1469.

Elagib, K.E., Mihaylov, I.S., Delehanty, L.L., Bullock, G.C., Ouma, K.D., Caronia, J.F., Gonias, S.L., and Goldfarb, A.N. (2008). Cross-talk of GATA-1 and P-TEFb in megakaryocyte differentiation. Blood *112*, 4884–4894.

Garriga, J., Xie, H., Obradovic, Z., and Graña, X. (2010). Selective control of gene expression by CDK9 in human cells. J. Cell. Physiol. *222*, 200–208.

Gekas, C., Rhodes, K.E., Gereige, L.M., Helgadottir, H., Ferrari, R., Kurdistani, S.K., Montecino-Rodriguez, E., Bassel-Duby, R., Olson, E.N., Krivtsov, A.V., et al. (2009). Mef2C is a lineage-restricted target of Scl/Tal1 and regulates megakaryopoiesis and B-cell homeostasis. Blood *113*, 3461–3471.

Gilles, L., Bluteau, D., Boukour, S., Chang, Y., Zhang, Y., Robert, T., Dessen, P., Debili, N., Bernard, O.A., Vainchenker, W., and Raslova, H. (2009). MAL/SRF complex is involved in platelet formation and megakaryocyte migration by regulating MYL9 (MLC2) and MMP9. Blood *114*, 4221–4232.

Halene, S., Gao, Y., Hahn, K., Massaro, S., Italiano, J.E., Jr., Schulz, V., Lin, S., Kupfer, G.M., and Krause, D.S. (2010). Serum response factor is an essential transcription factor in megakaryocytic maturation. Blood *116*, 1942–1950.

Hamlett, I., Draper, J., Strouboulis, J., Iborra, F., Porcher, C., and Vyas, P. (2008). Characterization of megakaryocyte GATA1-interacting proteins: the corepressor ETO2 and GATA1 interact to regulate terminal megakaryocyte maturation. Blood *112*, 2738–2749.

He, N., Pezda, A.C., and Zhou, Q. (2006). Modulation of a P-TEFb functional equilibrium for the global control of cell growth and differentiation. Mol. Cell. Biol. *26*, 7068–7076.

Heitzer, M.D., and DeFranco, D.B. (2006). Hic-5/ARA55, a LIM domain-containing nuclear receptor coactivator expressed in prostate stromal cells. Cancer Res. *66*, 7326–7333.

Jeronimo, C., Forget, D., Bouchard, A., Li, Q., Chua, G., Poitras, C., Thérien, C., Bergeron, D., Bourassa, S., Greenblatt, J., et al. (2007). Systematic analysis of the protein interaction network for the human transcription machinery reveals the identity of the 7SK capping enzyme. Mol. Cell *27*, 262–274.

Kadri, Z., Shimizu, R., Ohneda, O., Maouche-Chretien, L., Gisselbrecht, S., Yamamoto, M., Romeo, P.-H., Leboulch, P., and Chretien, S. (2009). Direct binding of pRb/E2F-2 to GATA-1 regulates maturation and terminal cell division during erythropoiesis. PLoS Biol. *7*, e1000123.

Klusmann, J.-H., Godinho, F.J., Heitmann, K., Maroz, A., Koch, M.L., Reinhardt, D., Orkin, S.H., and Li, Z. (2010). Developmental stage-specific interplay of GATA1 and IGF signaling in fetal megakaryopoiesis and leukemogenesis. Genes Dev. *24*, 1659–1672.

Krueger, B.J., Varzavand, K., Cooper, J.J., and Price, D.H. (2010). The mechanism of release of P-TEFb and HEXIM1 from the 7SK snRNP by viral and cellular activators includes a conformational change in 7SK. PLoS ONE *5*, e12335.

Kuwahara, K., Kinoshita, H., Kuwabara, Y., Nakagawa, Y., Usami, S., Minami, T., Yamada, Y., Fujiwara, M., and Nakao, K. (2010). Myocardin-related transcription factor A is a common mediator of mechanical stress- and neurohumoral stimulation-induced cardiac hypertrophic signaling leading to activation of brain natriuretic peptide gene expression. Mol. Cell. Biol. *30*, 4134–4148.

Li, Z., Godinho, F.J., Klusmann, J.-H., Garriga-Canut, M., Yu, C., and Orkin, S.H. (2005). Developmental stage-selective effect of somatically mutated leukemogenic transcription factor GATA1. Nat. Genet. *37*, 613–619.

Li, Y., Ma, J., Zhu, H., Singh, M., Hill, D., Greer, P.A., Arnold, J.M., Abel, E.D., and Peng, T. (2011). Targeted inhibition of calpain reduces myocardial hypertrophy and fibrosis in mouse models of type 1 diabetes. Diabetes *60*, 2985–2994.

Liu, Z., Yue, S., Chen, X., Kubin, T., and Braun, T. (2010). Regulation of cardiomyocyte polyploidy and multinucleation by CyclinG1. Circ. Res. *106*, 1498–1506.

Lordier, L., Jalil, A., Aurade, F., Larbret, F., Larghero, J., Debili, N., Vainchenker, W., and Chang, Y. (2008). Megakaryocyte endomitosis is a failure of late cytokinesis related to defects in the contractile ring and Rho/Rock signaling. Blood *112*, 3164–3174.

Michels, A.A., Fraldi, A., Li, Q., Adamson, T.E., Bonnet, F., Nguyen, V.T., Sedore, S.C., Price, J.P., Price, D.H., Lania, L., and Bensaude, O. (2004). Binding of the 7SK snRNA turns the HEXIM1 protein into a P-TEFb (CDK9/cyclin T) inhibitor. EMBO J. *23*, 2608–2619.

Mukhina, S., Wang, Y.L., and Murata-Hori, M. (2007). Alpha-actinin is required for tightly regulated remodeling of the actin cortical network during cytokinesis. Dev. Cell *13*, 554–565.

Muñoz, J.P., Collao, A., Chiong, M., Maldonado, C., Adasme, T., Carrasco, L., Ocaranza, P., Bravo, R., Gonzalez, L., Díaz-Araya, G., et al. (2009). The transcription factor MEF2C mediates cardiomyocyte hypertrophy induced by IGF-1 signaling. Biochem. Biophys. Res. Commun. *388*, 155–160.

Muntean, A.G., and Crispino, J.D. (2005). Differential requirements for the activation domain and FOG-interaction surface of GATA-1 in megakaryocyte gene expression and development. Blood *106*, 1223–1231.

Nakamura, F., Stossel, T.P., and Hartwig, J.H. (2011). The filamins organizers of cell structure and function. Cell Adh. Migr. *5*, 160–169.

Nelson, T.J., Balza, R., Jr., Xiao, Q., and Misra, R.P. (2005). SRF-dependent gene expression in isolated cardiomyocytes: regulation of genes involved in cardiac hypertrophy. J. Mol. Cell. Cardiol. *39*, 479–489.

Nishikii, H., Eto, K., Tamura, N., Hattori, K., Heissig, B., Kanaji, T., Sawaguchi, A., Goto, S., Ware, J., and Nakauchi, H. (2008). Metalloproteinase regulation improves in vitro generation of efficacious platelets from mouse embryonic stem cells. J. Exp. Med. *205*, 1917–1927.

Peterlin, B.M., and Price, D.H. (2006). Controlling the elongation phase of transcription with P-TEFb. Mol. Cell *23*, 297–305.

Pinto do O, P., Kolterud, A., and Carlsson, L. (1998). Expression of the LIM-homeobox gene LH2 generates immortalized steel factor-dependent multipotent hematopoietic precursors. EMBO J. *17*, 5744–5756.

Price, D.H. (2008). Poised polymerases: on your mark...get set...go! Mol. Cell *30*, 7–10.

Raslova, H., Kauffmann, A., Sekkaï, D., Ripoche, H., Larbret, F., Robert, T., Le Roux, D.T., Kroemer, G., Debili, N., Dessen, P., et al. (2007). Interrelation between polyploidization and megakaryocyte differentiation: a gene profiling approach. Blood *109*, 3225–3234.

Ridinger, H., Rutenberg, C., Lutz, D., Buness, A., Petersen, I., Amann, K., and Maercker, C. (2009). Expression and tissue localization of beta-catenin, alpha-actinin and chondroitin sulfate proteoglycan 6 is modulated during rat and human left ventricular hypertrophy. Exp. Mol. Pathol. *86*, 23–31.

Sano, M., and Schneider, M.D. (2004). Cyclin-dependent kinase-9: an RNAPII kinase at the nexus of cardiac growth and death cascades. Circ. Res. *95*, 867–876.

Sano, M., Abdellatif, M., Oh, H., Xie, M., Bagella, L., Giordano, A., Michael, L.H., DeMayo, F.J., and Schneider, M.D. (2002). Activation and function of cyclin T-Cdk9 (positive transcription elongation factor-b) in cardiac muscle-cell hypertrophy. Nat. Med. *8*, 1310–1317.

Sedore, S.C., Byers, S.A., Biglione, S., Price, J.P., Maury, W.J., and Price, D.H. (2007). Manipulation of P-TEFb control machinery by HIV: recruitment of P-TEFb from the large form by Tat and binding of HEXIM1 to TAR. Nucleic Acids Res. *35*, 4347–4358.

Smith, E.C., Thon, J.N., Devine, M.T., Lin, S., Schulz, V.P., Guo, Y., Massaro, S.A., Halene, S., Gallagher, P., Italiano, J.E., Jr., and Krause, D.S. (2012). MKL1 and MKL2 play redundant and crucial roles in megakaryocyte maturation and platelet formation. Blood *120*, 2317–2329.

Takano, E., Nosaka, T., Lee, W.J., Nakamura, K., Takahashi, T., Funaki, M., Okada, H., Hatanaka, M., and Maki, M. (1993). Molecular diversity of calpastatin in human erythroid cells. Arch. Biochem. Biophys. *303*, 349–354.

Tan, Y., Dourdin, N., Wu, C., De Veyra, T., Elce, J.S., and Greer, P.A. (2006). Conditional disruption of ubiquitous calpains in the mouse. Genesis *44*, 297–303.

Taneike, M., Mizote, I., Morita, T., Watanabe, T., Hikoso, S., Yamaguchi, O., Takeda, T., Oka, T., Tamai, T., Oyabu, J., et al. (2011). Calpain protects the heart from hemodynamic stress. J. Biol. Chem. *286*, 32170–32177.

Tiedt, R., Schomber, T., Hao-Shen, H., and Skoda, R.C. (2007). *Pf4-Cre* transgenic mice allow the generation of lineage-restricted gene knockouts for studying megakaryocyte and platelet function in vivo. Blood *109*, 1503–1506.

Wendt, A., Thompson, V.F., and Goll, D.E. (2004). Interaction of calpastatin with calpain: a review. Biol. Chem. *385*, 465–472.

Wickrema, A., and Crispino, J.D. (2007). Erythroid and megakaryocytic transformation. Oncogene *26*, 6803–6815.

Wu, J.-Q., Bähler, J., and Pringle, J.R. (2001). Roles of a fimbrin and an alpha-actinin-like protein in fission yeast cell polarization and cytokinesis. Mol. Biol. Cell *12*, 1061–1077.

Xu, Y., Bismar, T.A., Su, J., Xu, B., Kristiansen, G., Varga, Z., Teng, L., Ingber, D.E., Mammoto, A., Kumar, R., and Alaoui-Jamali, M.A. (2010). Filamin A regulates focal adhesion disassembly and suppresses breast cancer cell migration and invasion. J. Exp. Med. *207*, 2421–2437.

Xue, Y., Yang, Z., Chen, R., and Zhou, Q. (2010). A capping-independent function of MePCE in stabilizing 7SK snRNA and facilitating the assembly of 7SK snRNP. Nucleic Acids Res. *38*, 360–369.

Yamaguchi, O., Taneike, M., and Otsu, K. (2012). Cooperation between proteolytic systems in cardiomyocyte recycling. Cardiovasc. Res. *96*, 46–52.

Yik, J.H.N., Chen, R., Nishimura, R., Jennings, J.L., Link, A.J., and Zhou, Q. (2003). Inhibition of P-TEFb (CDK9/Cyclin T) kinase and RNA polymerase II transcription by the coordinated actions of HEXIM1 and 7SK snRNA. Mol. Cell *12*, 971–982.

Yund, E.E., Hill, J.A., and Keller, R.S. (2009). Hic-5 is required for fetal gene expression and cytoskeletal organization of neonatal cardiac myocytes. J. Mol. Cell. Cardiol. *47*, 520–527.

Zhou, Q., Li, T., and Price, D.H. (2012). RNA polymerase II elongation control. Annu. Rev. Biochem. *81*, 119–143.